Clinicopathologic, imaging and histologic features in cases of neurologic disease in psittacine birds

Ester Pintado, **Jaume Martorell**, **Ferran Solanes**, **Antonio J. Ramis**[1]

Servei de Diagnòstic de Patologia Veterinària, Universitat Autònoma de Barcelona, Bellaterra (Pintado, Ramis); IRTA, Centre de Recerca en Sanitat Animal (CReSA, IRTA-UAB), Bellaterra (Ramis); Hospital Clinic Veterinari, Facultat de Veterinaria, Universitat Autònoma de Barcelona, Bellaterra (Martorell, Solanes); Departament de Medicina i Cirurgia Animals, Facultat de Veterinaria, Universitat Autònoma de Barcelona, Bellaterra (Martorell)

[1]Corresponding author: Antonio J. Ramis, Universitat Autònoma de Barcelona, 08193 Bellaterra, Barcelona, Spain; antonio.ramis@uab.cat

Abstract

This report describes the use of magnetic resonance imaging to evaluate the central nervous system and the histopathological confirmation of the central nervous system lesions of three psittacine birds with neurologic signs. One bird presented recumbency due to a non-ambulatory paraparesis, and two birds presented ataxia and impaired proprioception. In all three cases, imaging was performed and infectious diseases were excluded in Cases 1 and 2. In Case 1, imaging showed a large mass arising from the left lung, in Case 2 a multinodular coelomic mass running from the left caudal pulmonary area to the left cranial renal pole, and in Case 3, a diffuse hyperintensity affecting the lumbar spinal cord. In the first two cases, both masses invaded the vertebral canal, causing spinal cord compression. All the birds were euthanized and a post mortem examination was performed in each case. The final diagnoses were pulmonary carcinoma in Cases 1 and 2, and granulomatous and lymphocytic leptomeningitis caused by *Mycobacterium genavense* in Case 3. This report shows the advantage of magnetic resonance imaging to enable visualization of the lesions where the nervous system is affected, and how histopathology can confirm the diagnosis of the imaging findings.

Running head: Psittacine neurologic diseases: imaging and pathologic features.

Keywords: histopathology, magnetic resonance image, mycobacteriosis, neoplasia, neurologic signs, psittacine.

Body of manuscript

The neurologic examination of birds is challenging because many of the tests designed to evaluate mammalian species are difficult to perform or interpret in avian species. Depending on the localization of the lesion, clinical signs of neurologic disease can vary from unspecific signs such as apathy and anorexia, to changes in the mental status, head tilt and nystagmus, muscular tremors, seizures, blindness, ataxia, lameness and total recumbency because of paresis or paraplegia.[3,8]

In psittacine birds, the most common neurologic disfunctions occurring in the central nervous system are infectious diseases of different etiology.[15,13] However, other alterations such as ingestion of toxic substances, metabolic or nutritional, trauma and congenital disorders should also be considered.[13] Furthermore, neoplasia is a common finding affecting primarily the central and peripheral nervous system, or even arising from other celomic organs and invading or compressing the spinal cord or sciatic nerves.[2,14,17,22,24] In cases where neoplasia affects the spinal cord or sciatic nerves, birds display unilateral to bilateral leg weakness, and slight ataxia or paralysis. However, sciatic nerve compression secondary to gonad, adrenal gland or kidney enlargement due to neoplasia or other problems should be included in the differential diagnosis.[8]

Magnetic resonance imaging (MRI) is a non-invasive process that provides excellent soft tissue contrast of the central nervous system (CNS) and spatial orientation of anatomic structures. It has been increasingly used in avian medicine for anatomical description of the brain[20] and also for the diagnosis of neurological diseases.[8] The present work provides a comparison between MRI findings and post-mortem examination in 3 cases of neurologic clinical disease in psittacine birds.

Three psittacine birds with neurologic signs were evaluated. After physical and neurologic examination, an MRI was performed. All three birds were premedicated with

butorphanol (1 mg/kg) and meloxicam (0.5 mg/kg). Anesthesia was induced with isoflurane 5% in oxygen, administered via a facemask, followed by endotracheal intubation and maintenance with isoflurane 2% in oxygen. MRI provided information to evaluate spinal cord abnormalities in the three cases. Due to bad prognosis, all birds were euthanized. A complete post-mortem examination of each bird was performed. Different representative samples of each case were collected and fixed in 10% neutral buffered formalin, embedded in paraffin, sectioned and stained with hematoxylin-eosin.

Case-1: A 24-year-old male Green winged macaw (*Ara chloroptera*) was presented with five-days history of recumbency. The owner found the bird lying on the ground, and although the bird could not stand up, it was able to eat. Physical examination revealed atrophy of the pectoral muscles and body condition score 1/5 with 890 g weight. Neurologic examination revealed non-ambulatory spastic symmetrical paraparesis and no apparent spinal hyperesthesia. Neuroanatomical location of the lesion was placed in the thoracic and cranial synsacrum spinal cord segment. Whole body radiographs showed a soft tissue opacity involving the left lung, which was caudally enlarged, compressing the left caudal thoracic air sac. Results of the complete blood count (CBC) were unremarkable. An MRI was performed to confirm spinal cord involvement. A large mass arising from the left lung was shown, infiltrating the vertebrae at the level of the fifth, sixth and seventh thoracic vertebrae of the synsacrum, invading the vertebral canal and causing spinal cord compression. The mass was heterogeneously hyperintense on T2-weighted images and slightly hyperintense on T1-weighted images. These findings were compatible with pulmonary neoplasia extending to the adjacent vertebrae and vertebral canal causing spinal cord compression. The autopsy revealed that the bird was in fairly poor body condition. The left lung was markedly enlarged with multiple, prominent, up to 1 mm in diameter, white to yellow nodules, distributed throughout the parenchyma It was firmly stuck to the adjacent thoracic spine and ribs and infiltration of

the vertebral bodies and the spinal canal was detected. Histologically, nearly 90% of the lung parenchyma was effaced by a multinodular, non-encapsulated, not demarcated, moderately cellular and highly infiltrative epithelial neoplasm which reached and replaced several vertebral bodies and transverse processes of thoracic vertebrae, and also invaded the spinal canal, compressing the spinal cord. The neoplastic cells grew in cords, papillae and large densely packed nests; they were cuboidal to cylindric in shape with distinct borders. Anisocytosis and anisokaryosis were moderate and the mitotic count (MC) was 45 mitoses in 2.37 mm^2. Occasionally, neoplastic cells showed small cilia at their apical pole. There were extensive areas of necrosis that multifocally underwent mineralization. The spinal cord showed multifocal and extensive areas of vacuolization of the parenchyma with axonal degeneration and spheroids due to compression. Lastly, neoplastic cells were seen within lymphatic vessels. Immunoperoxidase (IP) staining for cytokeratin (CK) AE1/AE3 was performed with cytoplasmic immunoreaction of the neoplastic cells (Figure 1: A-C; Suppl. Figure 1). These findings were consistent with a malignant epithelial lung neoplasm infiltrating the vertebral bones, invading the spinal canal and compressing the spinal cord.

Case 2: A 16-year-old male African grey parrot *(Psittacus erithacus)* was presented with lameness of the right leg, unable to stand up. Upon physical examination, the bird was bright, alert and showed good body condition (score 3/5 with 410 g weight). Neurologic examination revealed a conscious proprioception loss in the left leg, a delay in the right leg and a non-ambulatory spastic paraparesis, more severe in the right side. Neuroanatomical location of the lesion was in the spinal cord, thoracic and cranial synsacrum segment. Radiographs revealed a coelomic mass located in the cranial pole area of both kidneys and a soft tissue radiodensity mass at the caudal left lung area. Results of a CBC were unremarkable. An MRI was performed given the suspicion of spinal cord affection. A large multilobulated mass was identified in the left lung also involving the cranial aspect of the left

kidney, infiltrating adjacent vertebrae at the level of sixth thoracic vertebrae and seventh and eighth thoracic vertebrae of the synsacrum, causing spinal cord compression. Solid and cystic areas were identified inside the neoplasia. Also, round and small sized masses were identified, scattered through the parenchyma of both lungs, and showed heterogeneously hyperintense on T2-weighted images and hypointense on T1-weighted images. Contrast enhancement (gadolinium 0.2 mL/kg) was slight and peripherally distributed in the cystic areas. These findings were compatible with pulmonary or left kidney neoplasia extending to the adjacent vertebrae and vertebral canal causing spinal cord compression. The autopsy showed that the bird was in good body condition. The most relevant finding was a white to yellow and highly infiltrative mass arising from the left lung, reaching adjacent thoracic vertebral bodies and the 4th rib, and invading, compressing and displacing the thoracic and abdominal air sacs. Microscopically, it corresponded to a diffuse non-encapsulated, non-demarcated and highly infiltrative epithelial neoplastic proliferation. In the lung, neoplastic cells grew in a densely cellular solid pattern with no evident areas of necrosis. In the surrounding invaded tissues and organs (air sacs, aorta, vertebral bodies, spinal canal and spinal cord), the neoplastic proliferation showed a different growth pattern, consisting of monolayer tubules with a central lumen filled with eosinophilic amorphous material and foamy macrophages, over a thin loosely arranged fibrovascular stroma. Neoplastic cells were cuboidal, with distinct cell borders and cilia in their apical pole. There was moderate anisocytosis and anisokaryosis, and the MC was 65 mitoses in 2.37 mm^2. The same changes seen in Case 1 at the vertebrae and spinal cord were also seen in this bird. As in the previous case, an IP staining for CK AE1/AE3 was performed with evident cytoplasmic immunoreaction of neoplastic cells (Figure 1: D-F; Suppl. Figure 2). These findings were consistent with a malignant epithelial lung neoplasm infiltrating the vertebral bones, invading the spinal canal and compressing the spinal cord.

Case-3: A 17-year-old male Orange-winged parrot (*Amazona amazonica*) was presented with a one-month history of generalized weakness. Upon physical examination, the bird was mildly depressed with a body weight of 445 g and a body condition score of 3/5. General physical examination was unremarkable. Radiographs revealed hepatomegaly and increased opacity of the left and right caudal air sacs, compatible with airsacculitis. The blood test showed severe leukocytosis 76x10^9/L (reference range 6-11 x10^9/L), hyper-betaglobulinemia 14.2 g/L (reference range 3.8-7.6 g/L).[10] Liver and air sac biopsies taken from an endoscopy revealed granulomatous hepatitis and airsacculitis. A Ziehl-Neelsen (ZN) staining from the liver sample demonstrated the presence of intracellular acid-fast bacilli compatible with a mycobacterial infection. Initial treatment consisted of enrofloxacin 15 mg/kg/12h, azithromycin 40 mg/kg/24h and pentoxifylline 100 mg/kg/12h for one month. Two months later, the bird showed ataxia and proprioception delay in both legs. Neurologic examination revealed ambulatory paraparesis. An MRI was performed in which T2- weighted images showed a diffuse hyperintensity affecting the lumbar spinal cord, with more severity at the left side suggesting a spinal cord inflammatory process or edema. No other abnormalities were observed in the rest of the coelomic cavity. The post mortem examination showed that the bird was in poor body condition with patent muscular atrophy. The most relevant gross finding in the coelomic cavity was a mild to moderate thickening of the duodenum wall. Microscopically, the changes detected in the spinal cord by image techniques corresponded to mild multifocal and perivascular aggregates of histiocytes with a foamy cytoplasm, and fewer lymphocytes and plasma cells located in the leptomeninges; at the brain and leptomeninges there were perivascular cuffs of up to 6 cells thick composed of the same inflammatory cells. With regards to the other organs, the duodenum presented a marked thickening and blunting of the villi due to a massive infiltration of large histiocytes with foamy cytoplasm and some multinucleated giant cells in the lamina propria. There were also

multifocal histiocytic inflammatory infiltrates in the lung, the adipose tissue of the coelomic cavity, the pericardium, the spleen, the liver and adrenal glands. A ZN staining revealed intracytoplasmic acid-fast bacilli compatible with mycobacteria (Figure 2). Lastly, a direct PCR from frozen liver samples revealed *Mycobacterium spp.* neither avium nor tuberculous complex; furthermore, a bacterial culture in liquid medium for 3 weeks confirmed the presence of *Mycobacterium spp*. Neither an avium or tuberculous complex nor an rRNA sequencing had a 100% match of the 16S gen with *M. genavense* species. These findings allowed the diagnosis of multisystemic mycobacteriosis caused by *Mycobacterium genavense.*

We describe three cases of neurologic alterations in the rear limbs of psittacines. Ataxia and posterior paresis or paralysis is common in birds, especially in psittacines.[9] In all three cases, MRI allowed a more appropriated prognostication than radiography as has been suggested in other cases.[15] Furthermore, MRI made it possible to confirm the poor prognosis resulting in the decision to perform euthanasia.

The multilobular masses observed by MRI within the celomic cavity of Cases 1 and 2 and their infiltrative behavior accounted for a malignant neoplasia or an inflammatory process with a nodular pattern. The post-mortem examination of both birds revealed similar findings highly compatible with a malignant neoplasia effacing the left lung and widely infiltrating adjacent tissues, the thoracic vertebral spine reaching the spinal cord and inducing compressive degenerative changes, thereby causing the observed clinical signs such as paraparesis, in agreement with previous reports.[2,4] The microscopic findings are in accordance with previously reported pulmonary carcinomas arising from the lung[2,4,14] or the air sacs,[14] although the growth pattern and cellular features of both tumors were different. The growth pattern in Case 1 was arranged in multi-layered nests with areas of necrosis, whereas in Case 2, the MRI detected cystic cavities correlated with the abundant monolayer tubules with a central lumen detected at the surrounding soft tissues, air sacs and vertebral bone. Regarding

187 the cellular features, in Case 1, the neoplastic cells showed only occasional cilia, whereas it
188 was a common finding in Case 2. The difference between these two neoplasms could be a
189 consequence of different cellular origin: Case 1 being potentially of pulmonary origin and
190 Case 2 originated from the air sacs, as the appearance of the last one was similar to previously
191 reported air sac cystadenocarcinomas.[1,10,11] The differentiation between pulmonary carcinoma
192 and air sac cystadenocarcinoma is challenging: although infiltration of the humerus has been
193 reported as a constant finding in the air sac carcinomas. It has also been described in some
194 lung carcinomas.[2,6] In our case, we did not find changes in the humerus by MRI neither in
195 post-mortem examination in any of the birds and therefore we classified both tumors as
196 pulmonary carcinomas.

197 In Case 3, the MRI showed diffuse hyperintensity affecting the lumbar spinal cord,
198 with more severity at the left side. These changes histologically corresponded to a mild
199 multifocal histiocytic leptomeningitis of the spinal cord. Therefore, the detection of mild
200 changes in the MRI in this case, supports its utility for the diagnosis of central nervous
201 diseases in this species. The gross and histologic findings in this case are in accordance with
202 the only previous report of *M. genavense* infection involving the CNS of a parrot.[5] Lastly, a
203 culture from a liver sample confirmed *Mycobacterium genavense.* Infection of the CNS in
204 psittacine is usually part of a systemic process and the microscopic lesions are similar to other
205 affected organs.[14] Although the source and route of infection with *M. genavense* in the herein
206 presented case could not be determined, an oral route was suggested due to the presence of
207 severe gastrointestinal lesions. Nevertheless, moderate lesions were found affecting the
208 respiratory tract, so an aerogenic route could not be ruled out. Thereafter, an hematogenous
209 dissemination is a feasible explanation for the extension of the lesions to the CNS, as has been
210 suggested in other reports.[5,15]

The three cases presented here provide an example of the utility of the MRI for the diagnosis of different conditions inducing nervous clinical signs in psittacine birds. The author's opinion encourages the use of MRI for the a good and accurate diagnosis in psittacine birds with nervous clinical signs.

Acknowledgments

We thank Blanca Pérez and Aida Neira from the Servei de Diagnòstic de Patologia Veterinària, Universitat Autònoma de Barcelona for their technical assistance, and Caroline Idowu for revising the manuscript.

Declaration of conflicting interests

The authors declare no conflict of interest with respect to the research, authorship or publication of this manuscript.

Funding

The authors received no financial support for the research, authorship, and/or publication of this article.

Bibliography

1 Azmanis P, et al. A Complicated, Metastatic, Humeral Air Sac Cystadenocarcinoma in a Timneh African Grey Parrot (Psittacus erithacus timneh) . J Avian Med Surg 2013;27:38–43.

2 Baumgartner WA, et al. Bronchogenic Adenocarcinoma in a Hyacinth Macaw (Anodorhynchus hyacinthinus). J Avian Med Surg 2008;22:218–225.

3 Clippinger TL, et al. The Avian Neurologic Examination and Ancillary Neurodiagnostic Techniques: A Review Update. Vet Clin North Am - Exot Anim Pract 2007;10:803–836.

4 Fredholm D V., et al. Pulmonary Adenocarcinoma With Osseous Metastasis and Secondary Paresis in a Blue and Gold Macaw (Ara Ararauna) . J Zoo Wildl Med 2012;43:909–913.

5 Gomez G, et al. Granulomatous Encephalomyelitis and Intestinal Ganglionitis in a Spectacled Amazon Parrot (Amazona albifrons) Infected with Mycobacterium genavense. J Comp Pathol 2011;144:219–222.

6 Jones MP, et al. Pulmonary Carcinoma with Metastases in a Moluccan Cockatoo (Cacatua moluccensis). J. Avian Med. Surg. ;15:107–113.

7 Murphy BG, Shivaprasad HL. Ganglioneuroma of the brachial plexus in two cockatiels (Nymphicus hollandicus). Vet Pathol 2008;45:690–692.

8 Platt SR. Evaluating and Treating the Nervous System. In: Harrison GJ, Lightfoot TL, eds. Clinical Avian Medicine, Spix Publi. Palm Beach, Florida: Six Publishing, 2006:493–518.

9 Pollock CG. Implication of Mycobacteria in clinical disorders. In: Harrison GJ, Lightfoot TL, eds. Clinical Avian Medicine, Spix Publi. Palm Beach, Florida: Six Publishing, 2006:681–690.

10 Powers L V, et al. Axillary Cystadenocarcinoma in a Moluccan Cockatoo (Cacatua moluccensis) Published by : American Association of Avian Pathologists Stable URL : http://www.jstor.org/stable/1592495 Your use of the JSTOR archive indicates your acceptance of the Terms & Co. 2016;42:408–412.

11 Raidal SR, et al. Airsac cystadenocarcinomas in cockatoos. Aust Vet J 2006;84:213–216.

12 Robat CS, et al. Avian Oncology: Diseases, Diagnostics, and Therapeutics. Vet Clin North Am - Exot Anim Pract 2017;20:57–86.

13 Schmidt RE, et al. Nervous System. In: Pathology of Pet and Aviary Birds. Hoboken, NJ, USA: John Wiley & Sons, Inc., 2015:221–236.

14 Schmidt RE, et al. Pathology of Pet and Aviary Birds: Second Edition. Hoboken, NJ, USA: Wiley Blackwell, 2015: 1-1–298 doi:10.1002/9781118828007.

15 Stauber E, et al. Magnetic resonance imaging is superior to radiography in evaluating spinal cord trauma in three Bald Eagles (Haliaeetus leucocephalus). J Avian Med Surg 2007;21:196–200.

Figures

Figure 1. Case 1, Green winged macaw (*Ara chloroptera*) (**A-C**). **A**. Pulmonary mass (PM) detected macroscopically in the left lung. **B.** Spin Echo-T1 Magnetic MRI (sagital view). Pulmonary mass (PM) arising from the left lung, infiltrating the vertebrae at the level of the fifth, sixth and seventh thoracic vertebrae of the synsacrum, invading the vertebral canal and causing spinal cord (Sc) compression (asterisk). The mass was heterogeneously hyperintense on T1-weighted images. **C.** Histologic section of the PM with solid pattern and necrotic areas, showing positive IP staining for CK AE1/AE3 (inset). Case 2, African grey parrot (*Psittacus Erithacus*) (**D-F**). **D**. PM arising from the left lung, reaching and invading adjacent thoracic vertebral bodies and the 4th rib (heart, liver and gastrointestinal tract were removed). **E.** T2-weighted MRI (dorsal view). PM in the left lung (LL) involving also the cranial aspect of the left kidney (LK), infiltrating adjacent thoracic vertebrae (asterisk). Solid and cystic areas were identified inside the neoplasia. **F.** Histologic section of the PM with cystic growth pattern invading the vertebral bone (arrowhead), showing positive IP staining for CK AE1/AE3 (inset). Cr, cranial; H, heart; V, ventricle; RL, right lung; LL, left lung; RK, right kidney; LK, left kidney; PM, pulmonary mass.

Figure 2. Case 3, Orange-winged parrot (*Amazona amazonica*). T2- weighted MRI (transversal view). Diffuse hyperintensity affecting the lumbar spinal cord, with more severity at the left side (arrowhead). RK, right kidney; LK, left kidney.

Supplementary material

Supplementary Figure 1. Case 1, Green-winged macaw (*Ara chloroptera*). **A**. Dorsoventral radiograph. A soft tissue pulmonary mass (PM) involving the left lung can be observed, compressing the left caudal thoracic air sac. There was also increased opacity of the right lung (RL) and air sacs. **B**. Spin Echo-T1 Magnetic MRI (transversal view). Pulmonary mass (PM) arising from the left lung, infiltrating the vertebrae, invading the vertebral canal and causing spinal cord (Sc) compression (asterisk). **C**. Histologic section of the PM with solid pattern and necrotic areas effacing the trabecular bone of the spinous process, occupying part of the spinal canal. V, ventricle; RL, right lung; LL, left lung; PM, pulmonary mass.

Supplementary Figure 2. Case 2, African grey parrot (*Psittacus Erithacus*). **A.** Lateral radiograph. PM located in the cranial pole area of both kidneys and at the caudal left lung area (arrowheads). **B.** Transversal T1-weighted MRI showed a hypointense mass (PM) in the left lung infiltrating adjacent thoracic vertebrae (asterisk) and causing spinal cord compression. Cr, cranial; PM, pulmonary mass; RL, right lung; Li, liver; Pv, proventriculus.

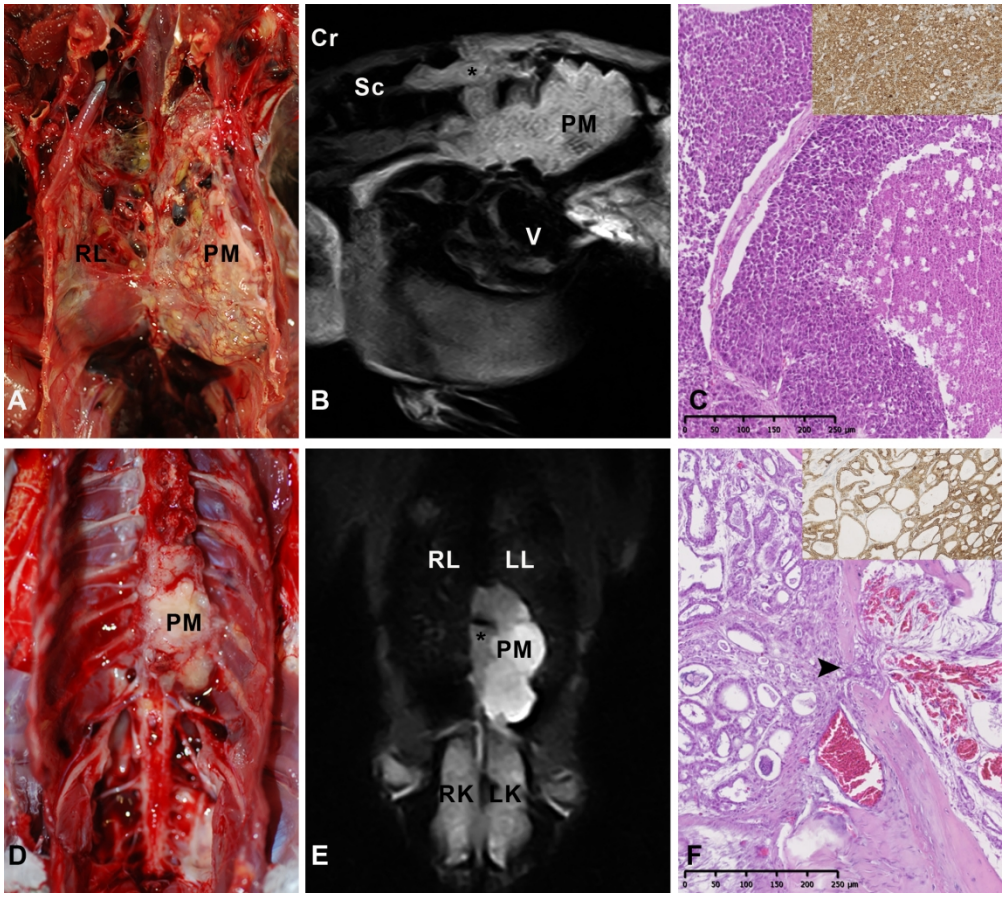

Figure 1

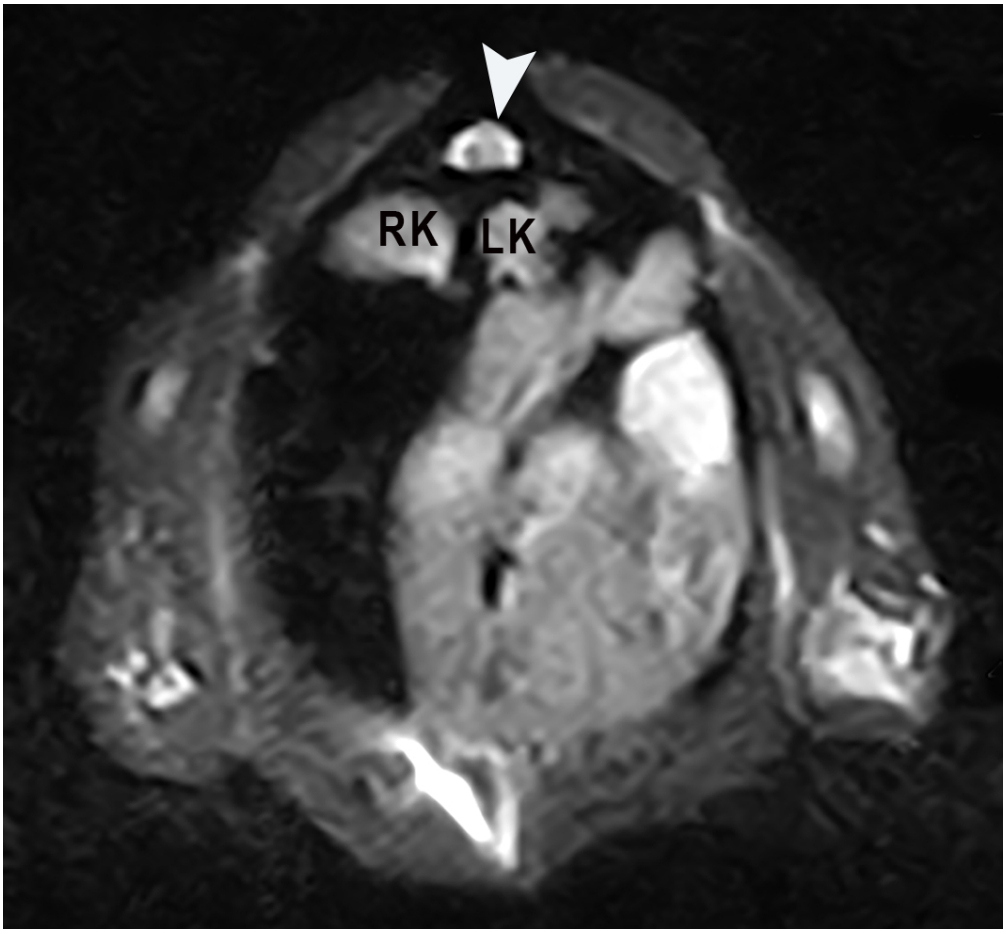

Figure 2

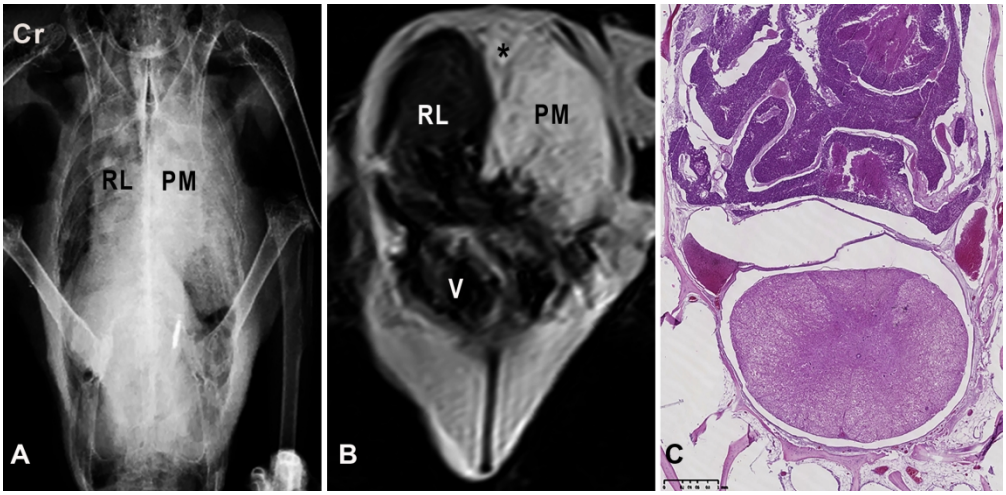
Cr
RL
PM
A
*
RL
PM
V
B
C

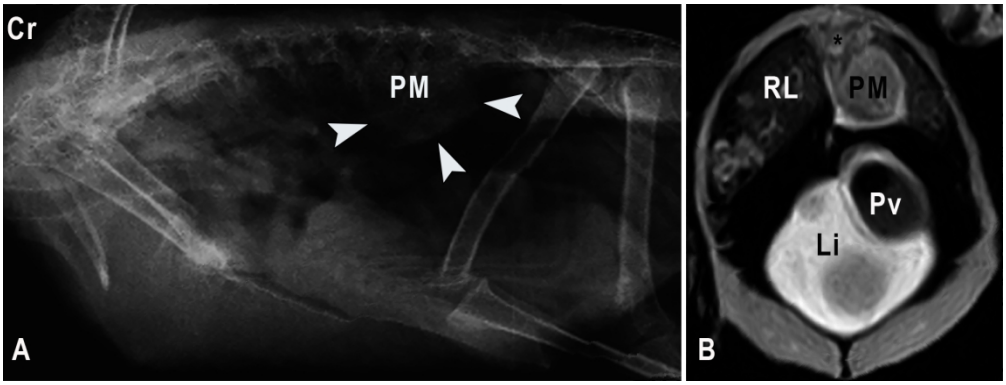
Cr
PM
A
*
RL
PM
Pv
Li
B